Received: 12 June 2024 | Revised: 1 September 2024 | Accepted: 1 September 2024

DOI: 10.1002/pc.29070

RESEARCH ARTICLE

Polymer COMPOSITES WILEY

Hygrothermal aging effects on the mechanical behaviors of twill-woven carbon fiber composite laminates with flame-retardant epoxy resin

Jinru Zhong[1] | **Junwei Ma**[1,2] | **Weikang Sun**[3] | **Zuxiang Lei**[1,2,4] | **Binbin Yin**[5]

[1]School of Civil Engineering and Architecture, East China Jiaotong University, Nanchang, Jiangxi, China

[2]State Key Laboratory of Performance Monitoring and Protecting of Rail Transit Infrastructure, East China Jiaotong University, Nanchang, China

[3]Department of Architecture and Civil Engineering, City University of Hong Kong, Kowloon, Hong Kong, China

[4]Engineering Research & Development Centre for Underground Technology of Jiangxi Province, East China Jiaotong University, Nanchang, China

[5]Department of Civil and Environmental Engineering, The Hong Kong Polytechnic University, Kowloon, Hong Kong, China

Correspondence
Zuxiang Lei, School of Civil Engineering and Architecture, East China Jiaotong University, Nanchang, 330013, Jiangxi, China.
Email: zxlei@ecjtu.edu.cn

Binbin Yin, Department of Civil and Environmental Engineering, The Hong Kong Polytechnic University, Kowloon, Hong Kong, China.
Email: binbin.yin@polyu.edu.hk

Funding information
National Natural Science Foundation of China; Primary Research and Development Plan of Jiangxi Province of China; Basic and Applied Basic Research Foundation of Guangdong Province

Abstract

Composite structures are frequently exposed to varying hygrothermal environments, which can lead to the deterioration of their mechanical properties. This study explores the effects of hygrothermal aging on the mechanical behaviors of twill-woven carbon fiber composite laminates, with a particular focus on laminates with flame-retardant epoxy resin (CF_FR)—a relatively underexplored area. The findings reveal several key insights: (1) CF_FR exhibit more pronounced aging damage compared to those with general epoxy resin (CF_G), primarily due to higher moisture absorption, which results in increased surface swelling and internal delamination. (2) Hygrothermal aging enhances the impact resistance of both types of laminates by increasing peak force, particularly at higher temperatures, thereby reducing impact-induced damage. (3) CF_FR suffers greater reductions in compressive and compression after impact (CAI) strength following aging, with CAI strength decreasing by 36.3% for flame-retardant laminates and 14.8% for CF_G after immersion at 70°C. (4) Significant local buckling is observed in the swollen regions of CF_FR under compressive loading, indicating an heightened vulnerability to structural instability after aging. These findings offer valuable insights into the performance of composite materials under prolonged moisture exposure, particularly in safety-critical applications where both flame retardancy and mechanical integrity are crucial.

Highlights

- More aging damage is captured from laminates with flame-retardant epoxy resin
- Aging temperatures alleviate LVI induced damage and improve the peak force
- Compressive and CAI strength are affected after prolonged aging conditions
- CAI strength of CF_FR decreases by 36.3% after exposure to the 70°C water bath
- Significant local buckling is observed in CF_FR under compressive loading

KEYWORDS

carbon fiber composite laminates, failure mechanisms, flame-retardant epoxy resin, Hygrothermal aging, mechanical performance

1 | INTRODUCTION

Carbon fiber reinforced polymers (CFRP) are increasingly utilized as structural components in aerospace, automotive, and marine applications due to their exceptional strength-to-weight ratios and superior corrosion resistance compared to conventional metallic materials.[1] However, during service, CFRP may be exposed to harsh environmental conditions that can alter their mechanical and physical properties.[2] This is particularly relevant for CFRP coated with flame-retardant epoxy resin, which enhances fire resistance, making them ideal for high-speed trains and other safety-critical applications where both flame retardancy and mechanical integrity are crucial. These materials often operate in hot and humid environments, which can exacerbate their degradation. Moreover, due to the inherently weak interlaminar properties of composites, even relatively low-impact loads may cause barely visible impact damage, leading to a reduction in the structural integrity of the laminate, such as a loss in compressive strength.[3–7] Therefore, understanding the aging mechanisms and impact resistance of these materials after prolonged exposure to hygrothermal conditions is essential for improving their long-term performance and reliability in real-world applications.

The mechanical properties and performance of CFRP are highly susceptible to the effects of the hygrothermal environment in their service life, and this phenomenon has been widely studied. The moisture absorption behavior of composites primarily involves two main mechanisms: (1) moisture absorption occurs through capillary action within the microcracks and voids of composites, and (2) water molecules bind with epoxy resins through hydrogen bonding, increasing the segment mobility.[8] The absorbed moisture acts as a plasticizer, reducing the glass transition temperature of the matrix,[9,10] thus influencing the overall performance of the laminates. While carbon fibers used as reinforcements exhibit minimal moisture absorption behavior and are less sensitive to moisture and temperature compared to the polymer matrix,[11] the significant mismatch in hygrothermal expansion between the matrix and fiber, due to differences in moisture absorption and thermal resistance, induces localized stress within the composites. This stress can lead to crack initiation and propagation in the matrix,[12] delamination, and weakening of the fiber/matrix interface,[13] ultimately compromising the mechanical properties of the materials.[14,15] Ray[13] identified that during environmental aging, adhesive damage at the fiber/matrix interface and the loss of interfacial integrity are the dominant damage mechanisms in polymer composites. Furthermore, they found that higher temperatures not only increase the rate of moisture uptake but also significantly reduce the shear strength of laminates. Liu et al.[2] demonstrated that hygrothermal environments cause local epoxy degradation, leading to cracks formation in the specimens during the aging process, which ultimately results in a decrease in compression strength. Ameer et al.[16] investigated the interdependence of moisture regain, hydrophobic treatment, and the mechanical properties of jute fiber-reinforced composites, concluding that the mechanical properties of the developed composite degrade linearly with immersion time. Although extensive research has been conducted on the hygrothermal aging mechanisms of composites, relatively few studies have investigated the moisture absorption behavior of flame-retardant epoxy resin.

It is crucial to examine the capability of laminate composites in structural applications to withstand impact resistance and damage tolerance, as even relatively low impact loads can lead to a remarkable degradation of the mechanical properties. Consequently, extensive research has been carried out on the low-velocity impact (LVI) tests[17–22] and compression after impact (CAI) tests[23–27] of composite materials. However, comparatively less attention has been paid to the influences of hygrothermal aging on CFRP's impact resistance. Khashaba et al.[28] performed the LVI tests on CFRP composite laminates and analyzed their residual compressive strength, considering the effects of different test temperatures. Raponi et al.[29] investigated the LVI behavior of twill flax/epoxy composites across a large range of temperatures and assessed the impact of these temperatures on their residual flexural properties. Karahan et al.[30] explored the LVI characteristics and damage in sandwich composites with four different core thicknesses in three-dimensional (3D) structures. Additionally, the effects of the weaving structure and hybridization on the LVI properties were investigated by Karahan et al.[31] Othman[32] investigated the influence of water immersion conditions on the LVI behavior of CFRP composites, finding that moist composites exhibited a more significant reduction in damage compared to dry ones. Zhong et al.[33] demonstrated that under moisture and cyclic hygrothermal conditions,

moisture can greatly alleviate the impact-induced damage in unidirectional CFRP laminates. Dogan et al.[34] examined the impacts of different temperatures during hygrothermal aging on the tensile properties, impact behavior, and CAI behavior of composites. Despite these studies, there is still limited research exploring the effects of hygrothermal conditioning at different temperatures on the mechanical performance (including LVI and CAI behaviors) of CFRP composite laminates with flame-retardant epoxy resin.

In this work, the aging mechanism, as well as the LVI and CAI behaviors of the twill woven carbon fiber reinforced flame-retardant epoxy resin composite laminates, were experimentally investigated. The surface and cross-sectional microstructures of laminates aged at varying temperatures were characterized using ultrasonic C-mode scanning (C-scan) and scanning electron microscopy (SEM) to reveal the material's microstructure evolution during the aging process. The impact responses, damage morphology and CAI strength of specimens were assessed through LVI and CAI tests to illustrate the effects of aging temperatures on these mechanical behaviors.

2 | MATERIALS AND METHODS

2.1 | Material and specimen fabrication

The specimens used in the experiments were fabricated from twill-woven carbon prepregs (T300-3 K carbon), as detailed in Table 1. The prepregs utilized both general and flame-retardant epoxy resin as the matrix materials. To fabricate the specimens, 24 layers of twill woven carbon fiber prepreg, incorporating with these two kinds of epoxy resin, were stacked in the same direction and placed into a mold. The curing process involved heating from 25°C to 145°C at a pressure of 0.001 MPa, followed by an increase in pressure to 0.005 MPa for 3 minutes, and then to 0.6 MPa for 80 min, as detailed in Figure 1A. After natural cooling to room temperature, the plates were cut into specimens measuring 100 mm × 100 mm × 4.8 mm (Figure 1C). The laminates made with general epoxy resin and flame-retardant epoxy resin are abbreviated to CF_G and CF_FR, respectively. To ensure the reliability of the data, each test was conducted at least three times.

TABLE 1 The parameters of twill woven carbon prepregs with different epoxy resins.

Prepreg	Fiber-weight content (%)	Areal density (g/m^2)	Thickness (mm)	Tg (°C)
With general epoxy resin	60	330	0.22	125–130
With flame-retardant epoxy resin	60	330	0.22	130–135

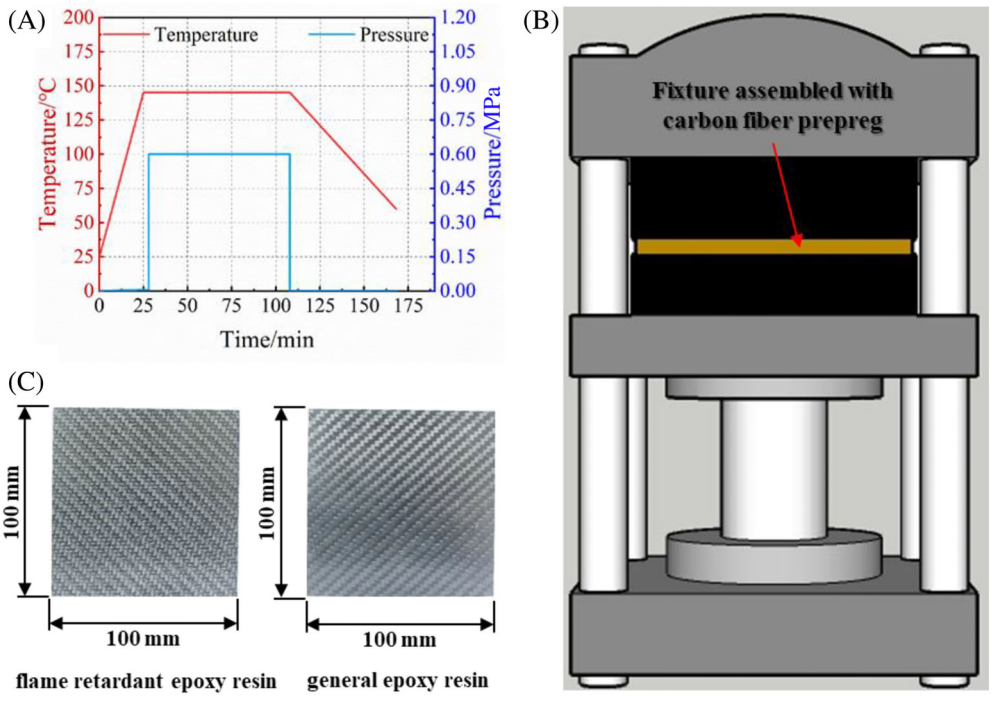

FIGURE 1 Fabrication of laminates: (A) cure conditions, (B) schematic of hot-press, (C) laminate samples.

Different methods of preparing the laminate can give rise to slight differences in the calculation of the fiber volume fraction.[16,35] In this study, the fiber volume fraction (V_f) was determined based on the prepreg weight and plate thickness using the following equation:

$$V_f = \frac{n \times m}{\rho \times h} \omega_f \quad (1)$$

where n is the number of prepreg plies, m is the areal density of the prepreg, ρ is the fiber density, h is the plate thickness, and ω_f is the fiber-weight content. V_f was consistently maintained at 0.62 across all the composite samples.

2.2 | Moisture absorption tests

Moisture absorption tests were performed in accordance with ASTM D5229/D5229M-20 to monitor the change in weight of the specimens over time. Prior to the moisture absorption experiments, all specimens were dried in an oven at 50°C to remove residual moisture until no further change in weight was observed. The dry weight of each specimen was then measured as a reference. Subsequently, the specimens were immersed in the water bath at 30°C, 50°C, and 70°C until they reached effective moisture equilibrium. An analytical balance, with an accuracy of ±0.1 mg, was employed to measure the weight of the specimens at regular intervals during the conditioning process, ensuring accurate tracking of moisture absorption. The moisture absorbed by specimens, expressed as a percentage of weight, can be calculated by the formula:

$$M(\%) = \frac{W_i - W_o}{W_o} \times 100 \quad (2)$$

where W_i denotes the mass of the specimen at the current time, and W_o is the mass of the oven-dry sample. In addition, the damage induced by moisture absorption under different hygrothermal aging conditions was evaluated using ultrasonic C-scan and SEM techniques.

2.3 | LVI tests

The LVI tests, conducted in accordance with ASTM D7136/D7136M, were carried out using a drop weight testing machine (INSTRON 9340). This machine was equipped with a hemispherical impactor weighing 5.337 kg and measuring 16 mm in diameter. As shown in Figure 2A, the specimen was secured by a support fixture, creating an unsupported circular area with a

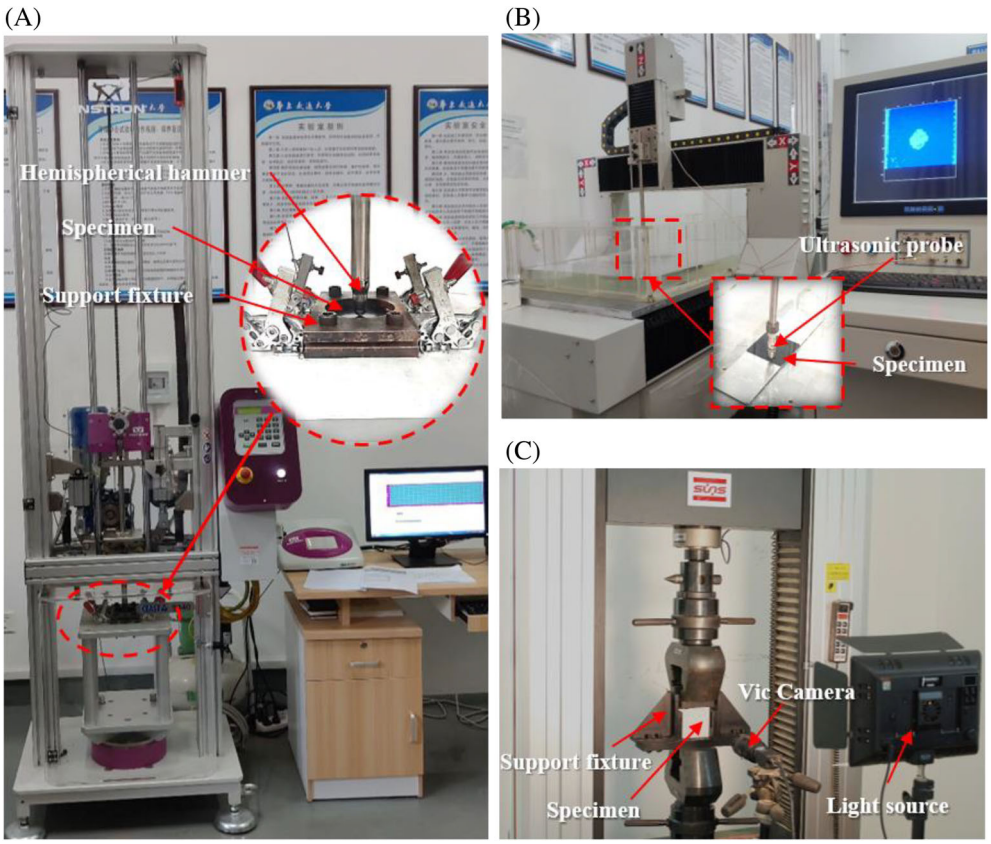

FIGURE 2 Devices for (A) LVI test, (B) ultrasound C-scan test and (C) CAI test.

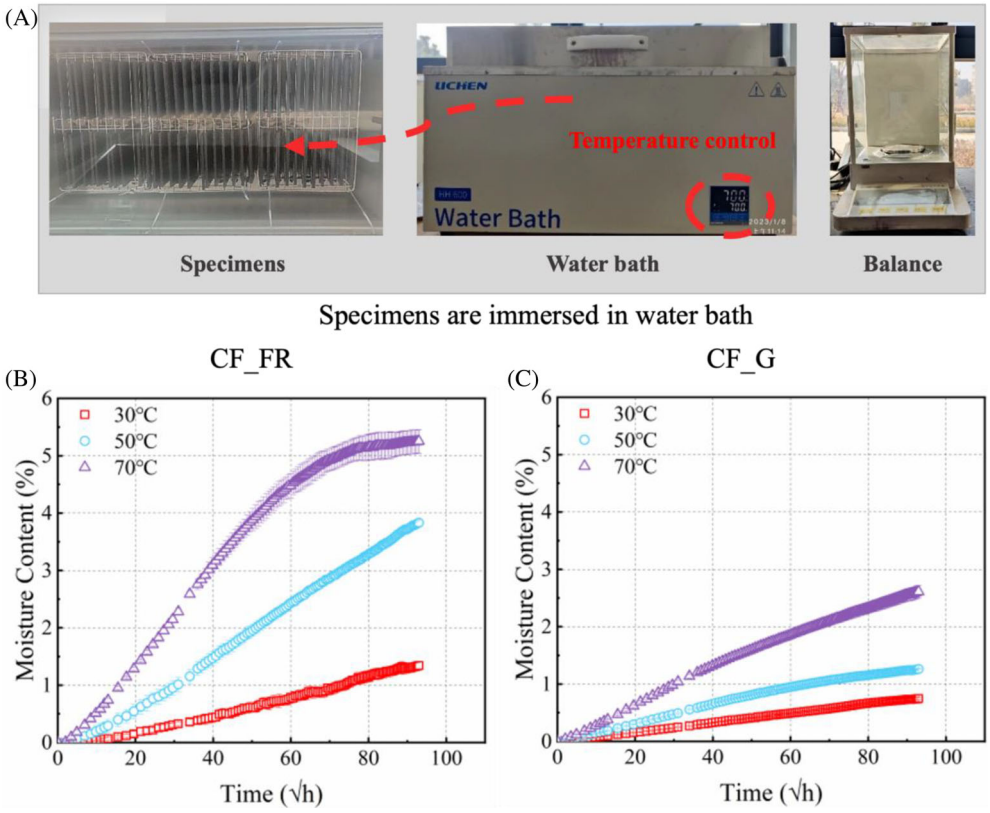

FIGURE 3 Moisture absorption behavior: (A) Specimens in water bath; (B) CF_FR and (C) CF_G specimens exposed to water with different temperatures for 360 days.

diameter of 75 mm. Three specimens from each aging condition were tested and subjected to an impact energy of 30 J. Time histories of the impact force, velocity, acceleration, and displacement were recorded. The damage resulting from LVI was assessed through an ultrasonic C-scan, as depicted in Figure 2B. Additionally, the damage morphologies were captured by using SEM.

2.4 | CAI tests

CAI tests were performed in accordance with ASTM D7137/D7137M through a SUNS electronic universal testing machine to assess the residual compression strength of the specimens. The CAI test setup, illustrated in Figure 2C, was used to record the corresponding compressive load–displacement data. Additionally, full-field strain during compressive loading was monitored using a VIC-2D system.

3 | RESULTS AND DISCUSSION

3.1 | Moisture absorption

To investigate the moisture absorption behavior of composite laminates, specimens were immersed in water baths at different temperatures, as shown in Figure 3A.

TABLE 2 Final content of moisture absorption at different hygrothermal conditions.

Laminates	Immersion temperatures (°C)	Aging time (days)	*M* (%)
CF_FR	30	360	1.34
	50	360	3.83
	70	360	5.25
CF_G	30	360	0.75
	50	360	1.26
	70	360	2.61

The moisture absorption curves in Figure 3B,C shows an initial linear increase in moisture content relative to the square root of time, indicating that moisture is easily absorbed into the epoxy resin during the early stages. Subsequently, the rate of moisture absorption gradually decreases, likely due to the progressive occupation of unsaturated voids and water molecule-binding sites within the laminates. Eventually, the moisture content stabilizes. The final content of moisture absorption of both types of laminates at various aging temperatures is illustrated in Table 2. It is evident that the moisture content of the two types of laminates is noticeably affected by the temperature of hygrothermal conditioning. The

moisture content of CF_FR increases from 1.34% to 5.25%, and that of CF_G increases from 0.75% to 2.61% as the temperature rises from 30°C to 70°C. Notably, only the CF_FR specimens reached an effective moisture equilibrium after immersion in water at 70°C for 360 days. This clearly indicates that the moisture content of the CF_FR samples is substantially higher than that of the CF_G samples under the same hygrothermal conditioning, suggesting that CF_FR may be more susceptible to damage caused by hygrothermal aging due to their greater capacity for moisture absorption.

3.2 | Surface morphology and microstructures after hygrothermal aging

In order to characterize the damage caused by hygrothermal aging, an attempt is made in this study to detect the surface morphology and microstructure of the two types of laminates using ultrasonic C-scan and SEM. Figure 4 illustrates the surface morphology and C-scan results for both laminates at different temperatures. It is evident that the degree of surface damage increases for both laminates as hygrothermal aging temperatures rise. Notably, the CF_FR specimens exhibit significantly more severe surface damage, consistent with the earlier observations regarding the moisture absorption behavior of these laminates. Moreover, at 50°C and 70°C, slight bulging areas are observed at the fiber intersections in the CF_G specimens, while the CF_FR specimens exhibit several distinct swelling areas on the surface. This indicates that the stress induced by hygrothermal aging at the fiber intersections may be greater than that in the surrounding regions, making these intersections more prone to the formation of swelling zone. Additionally, it is preliminarily confirmed that CF_FR is more susceptible to damage from hygrothermal aging than CF_G.

Moisture absorbed in hygrothermal aging environments can give rise to crack initiation and propagation, significant weakening at the fiber-matrix interface, and swelling of the laminate, all of which affect the internal microstructure of the laminate. The cross-sectional SEM images under various hygrothermal conditions are illustrated in Figure 5. While the interfaces between fiber and matrix are tightly bonded in the unaged specimens, moisture absorption over time can damage these interfaces, resulting in matrix cracking. This damage is likely due to the mismatched moisture absorption and thermal expansion capabilities between the different material phases (fiber and matrix). As the temperature of hygrothermal aging increases, laminates experience

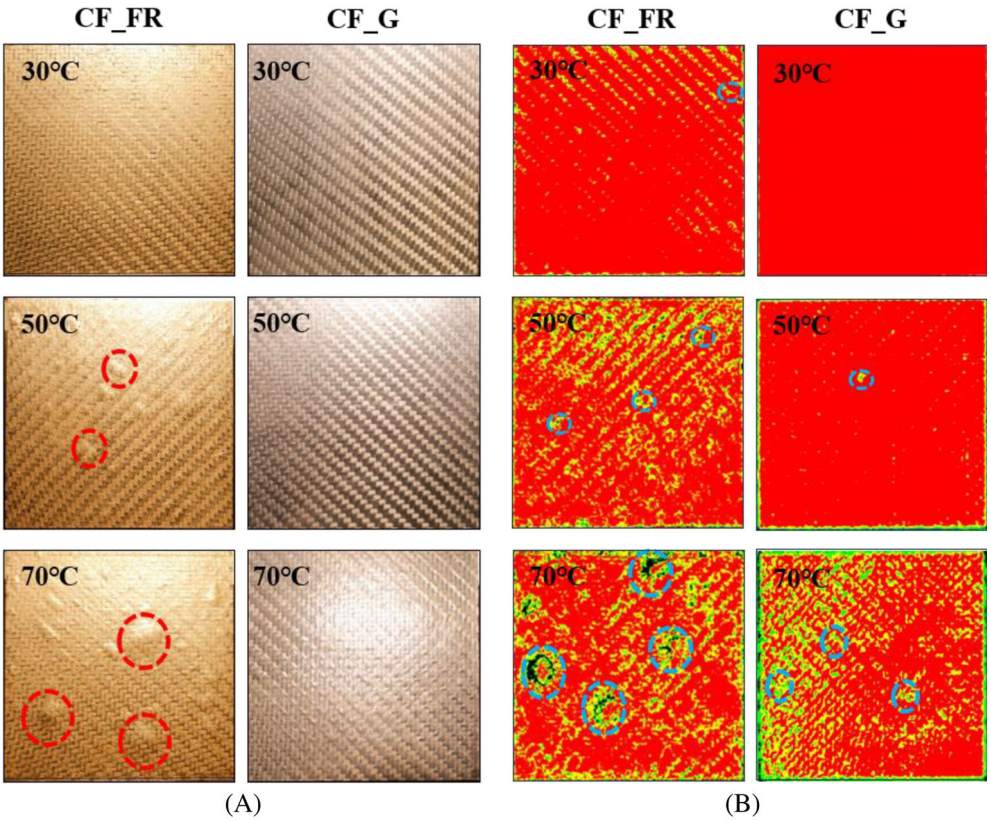

FIGURE 4 (A) Surface damage images and (B) C-Scan results after hygrothermal conditioning with different temperatures.

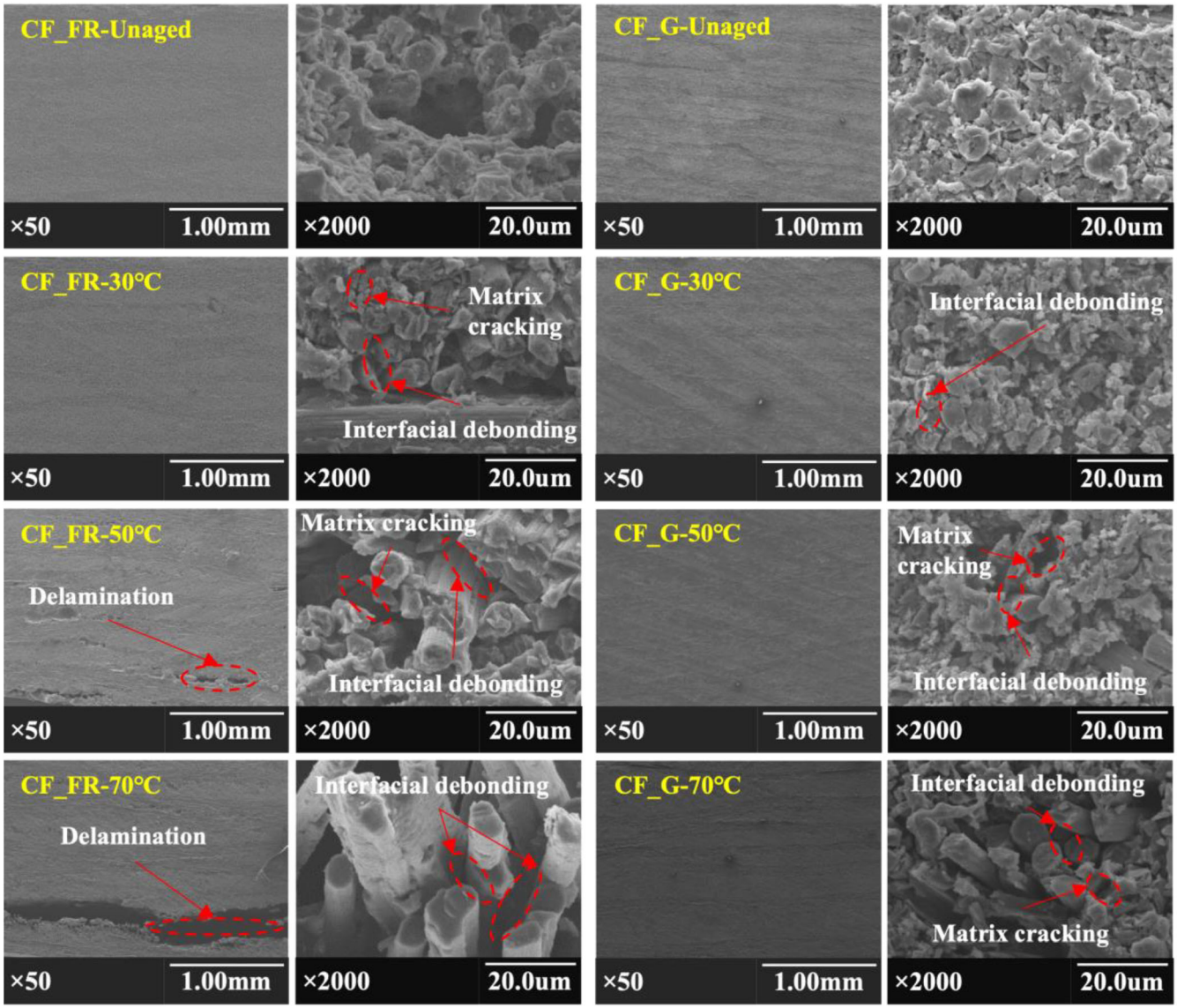

FIGURE 5 Cross sections of SEM images: (A) CF_FR subjected to various temperatures for water immersion; (B) CF_G subjected to various temperatures for water immersion.

more severe damage. Interfacial debonding is observed in both laminates after immersion at 30°C, suggesting that their microstructures may have been compromised, which could lead to a significant decline in mechanical properties, even in the absence of obvious surface swelling at this relatively low aging temperature. Furthermore, at higher temperatures, CF_FR exhibit more pronounced delamination damage compared to CF_G, which may be associated with much higher moisture content. Prolonged exposure of the CF_FR specimens to elevated temperatures during hygrothermal aging can increase hygrothermal stress, which promotes the generation and expansion of cracks, ultimately leading to irreversible delamination damage.

3.3 | LVI behavior

During the LVI tests, impact force versus time and displacements were recorded to evaluate the impact resistance of the materials. Figure 6 presents the impact responses at 30 J for the two composite laminates subjected to different hygrothermal aging conditions. It can be observed that the force-time curves for the samples soaked in water at different temperatures are similar to those of the unaged samples. Except for the specimens immersed at 30°C, the force corresponding to the initial point of damage induced by the impact is lower for both laminates, and it decreases with increasing temperature. This suggests that the initial impact damage occurs earlier

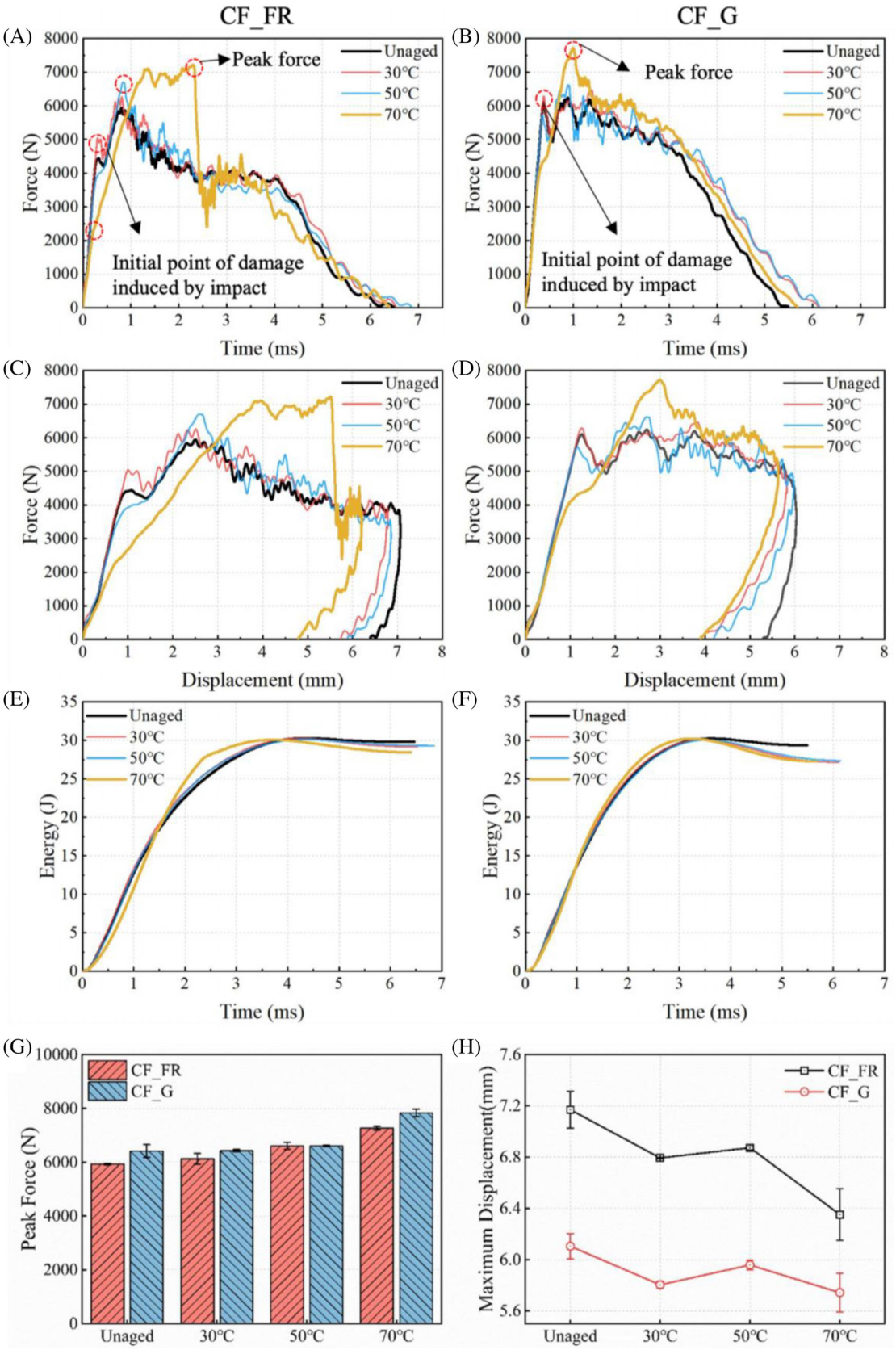

FIGURE 6 Impact responses at 30 J subjected to different hygrothermal aging conditions: (A) force versus time for CF_FR; (B) force versus time for CF_G; (C) force versus displacement for CF_FR; (D) force versus displacement for CF_G; (E) energy versus force for CF_FR; (F) energy versus force for CF_G; (G) peek force of two composite laminates, and (H) maximum displacement of two composite laminates.

when the laminate is subjected to impact loading, likely due to the higher degree of aging damage resulting from prolonged exposure to elevated temperatures. Interestingly, a remarkable increase in peak force is observed for both types of laminates conditioned at three temperatures compared to the unaged specimens, with the peak force increasing as the aging temperature rises. This increase may be related to the extent of swelling. Additionally, it is observed that the peak force of CF_FR appears later and remains oscillatory for a longer period compared to CF_G. This indicates that CF_FR specimens, with greater capacity for water absorption, can maintain their strength for a longer duration during impact.

Rebound takes place in all specimens, as detailed in the force-displacement curves illustrated in Figure 6C,D. The force–displacement curves for both laminates exhibit

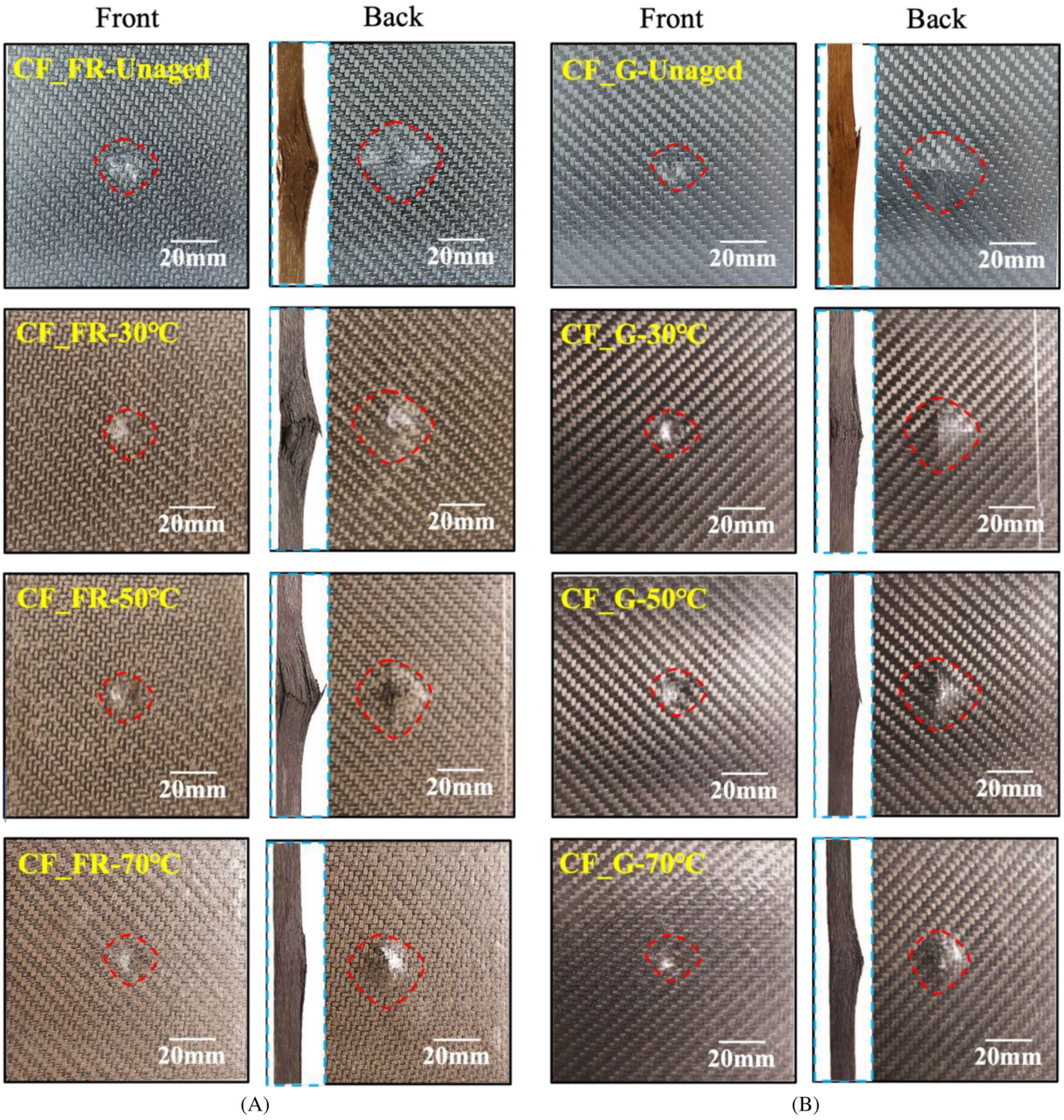

FIGURE 7 Impact damage morphologies of: (A) CF_FR at different water immersion aging temperatures and (B) GF_G at different water immersion aging temperatures under an impact energy of 30 J.

similar behavior at 30°C and 50°C. However, at the immersion temperature of 70°C, the linear stage of the curves is significantly shortened for both laminates, indicating that initial damage from the impact occurs with minimal deformation. In addition, the stiffness, represented by the linear stage of force–displacement curves, decreases for CF_FR at 70°C, while it remains relatively constant at temperatures below 70°C. This suggests that the integrity and the out-of-plane stiffness of CF_FR decrease obviously after prolonged exposure to a hygrothermal environment at higher temperatures. From the energy-time curves shown in Figure 6E,F, it is evident that the laminates under different hygrothermal aging conditions absorbed less energy than the unaged specimen, indicating that the extent of the damage may be smaller for the aged laminates. This observation is further corroborated by the results shown in Figure 8. A comparison of the peak force and maximum displacement of the two laminates after hygrothermal aging is depicted in Figure 6G,H. It is evident that the peak force of both laminates increases with temperature compared to the unaged sample, suggesting that laminates immersed at higher temperatures can better withstand higher impact loads. Specifically, CF_FR specimens show an increase in peak force ranging from 3.3% to 22.7% as the temperature increases from 30°C to 70°C, while CF_G specimens show an increase in peak force ranging from 0.2% to 22.1%, indicating that CF_FR shows a greater improvement in the resistance to impact loading under the same hygrothermal aging conditions. In addition, the maximum displacements of the two laminates are reduced after hygrothermal aging compared to the unaged specimens, indicating that the specimens can support higher impact loads with a lower maximum displacement.

The impact damage morphologies under an impact energy of 30 J at different aging temperatures are shown in Figure 7. As expected, the overall impact damage pattern remains unchanged across various conditioning temperatures. For both laminates, an indentation is observed on the front side, while a cross-shaped failure is evident on the rear side. Notably, the size of the indentation on the front surface and the cross-shaped failure on the back surface decrease significantly with increasing hygrothermal aging temperatures. Therefore, it can be concluded that the impact damage in laminates conditioned at different hygrothermal aging environments is reduced under LVI, with the reduction being more pronounced at higher temperatures. This effect may be related to the varying degrees of swelling of the laminates, resulting from differences in moisture absorption during the different hygrothermal aging conditions.

Figure 8 illustrates the C-scan detection results for impact-damaged areas of the two laminates conditioned at different hygrothermal aging temperatures. It is

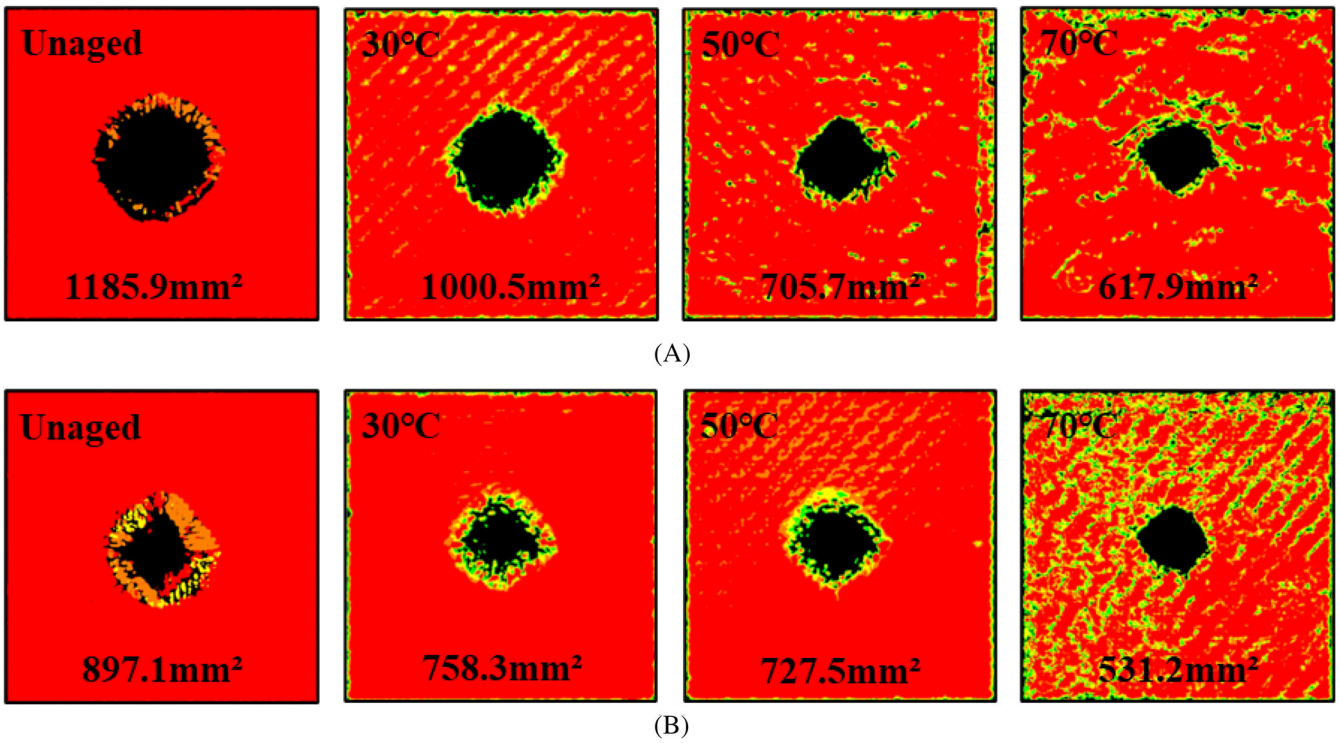

FIGURE 8 C-scan inspections: (A) CF_FR at different temperatures of immersion, and (B) CF_G at different temperatures of immersion.

evident that the damage zones in both laminates become more localized, forming an approximate diamond shape centered at the impact point. The size of the damage area decreases with increasing temperature, indicating that hygrothermal aging positively influences the reduction of impact damage, in line with the energy-time results shown in Figure 6E,F. Particularly, at 70°C, the damaged area of CF_FR decreased significantly by 47.9%, while CF_G showed a relatively smaller decrease of 40.8%. This variation may be attributed to the different moisture absorption capacities of the two epoxy resins. CF_FR, with its higher water absorption, likely experiences more significant swelling, which helps resist impact damage. A detailed microstructural examination of the cross-sections of samples carried out to assess the damage mechanisms in woven laminates conditioned at various hygrothermal temperatures, will be presented and discussed in the following section.

Figure 9 shows SEM microstructures of the cross-sections for the two types of composite laminates after being subjected to an impact energy of 30 J under various hygrothermal conditions. The SEM images reveal damage mechanisms, including delamination and fiber breakage, across all specimens, indicating that these are the principal damage modes under LVI. Furthermore, as the water bath temperature increases, a decrease in the degree of fiber breakage is observed in CF_FR, accompanied by more pronounced delamination damage. This shift is

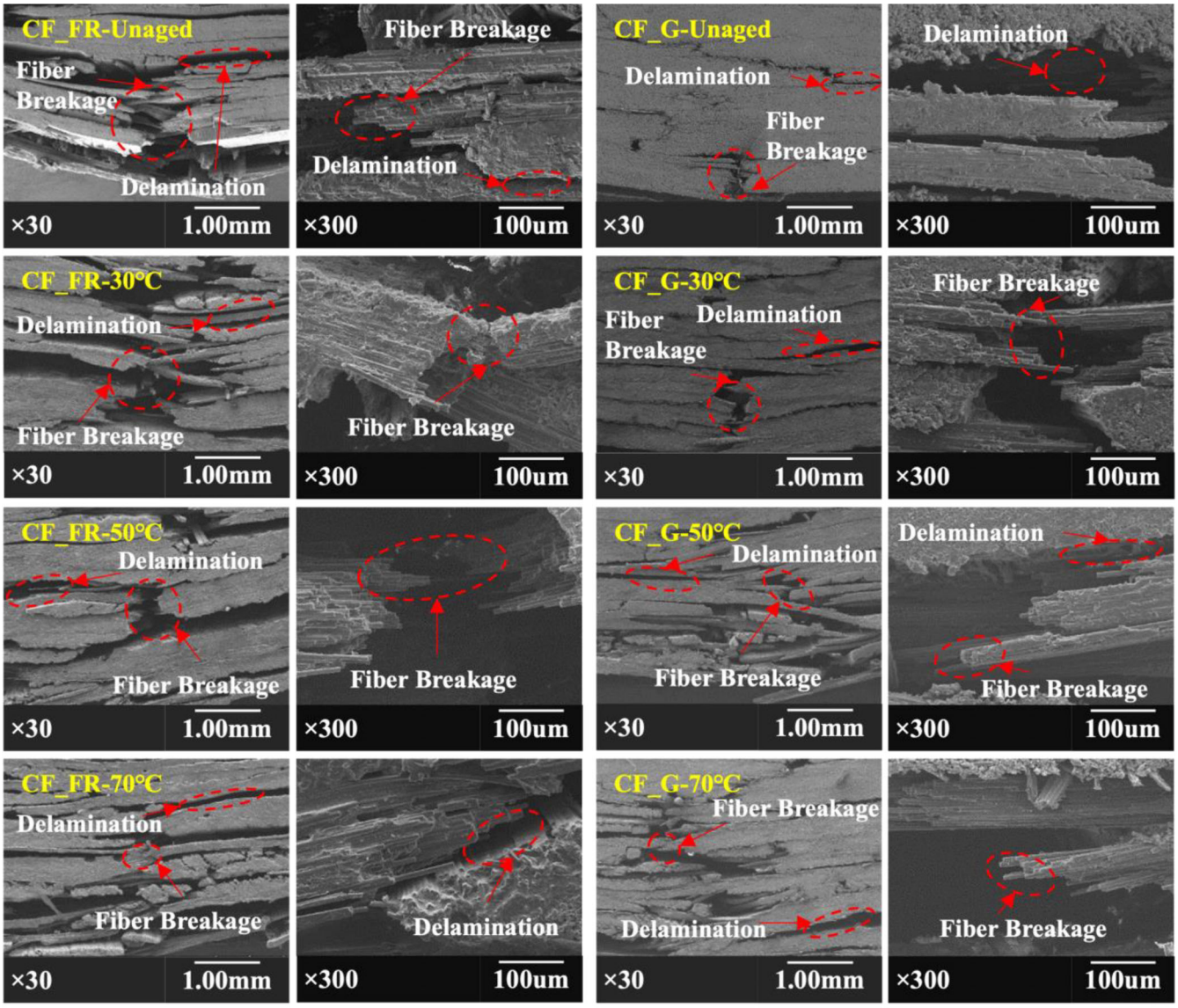

FIGURE 9 SEM fractographies of cross-section for (A) CF_FR after an impact energy of 30 J under various hygrothermal conditions and (B) CF_G after an impact energy of 30 J under various hygrothermal conditions.

likely due to CF_FR absorbing significant amounts of moisture during prolonged hygrothermal aging, leading to degradation at the fiber-matrix interface and resulting in increased delamination damage. Laminates with such damage are more susceptible to delamination when subjected to impact loads. In contrast, CF_G exhibits more concentrated fiber breakage upon impact, likely due to its lower moisture absorption.

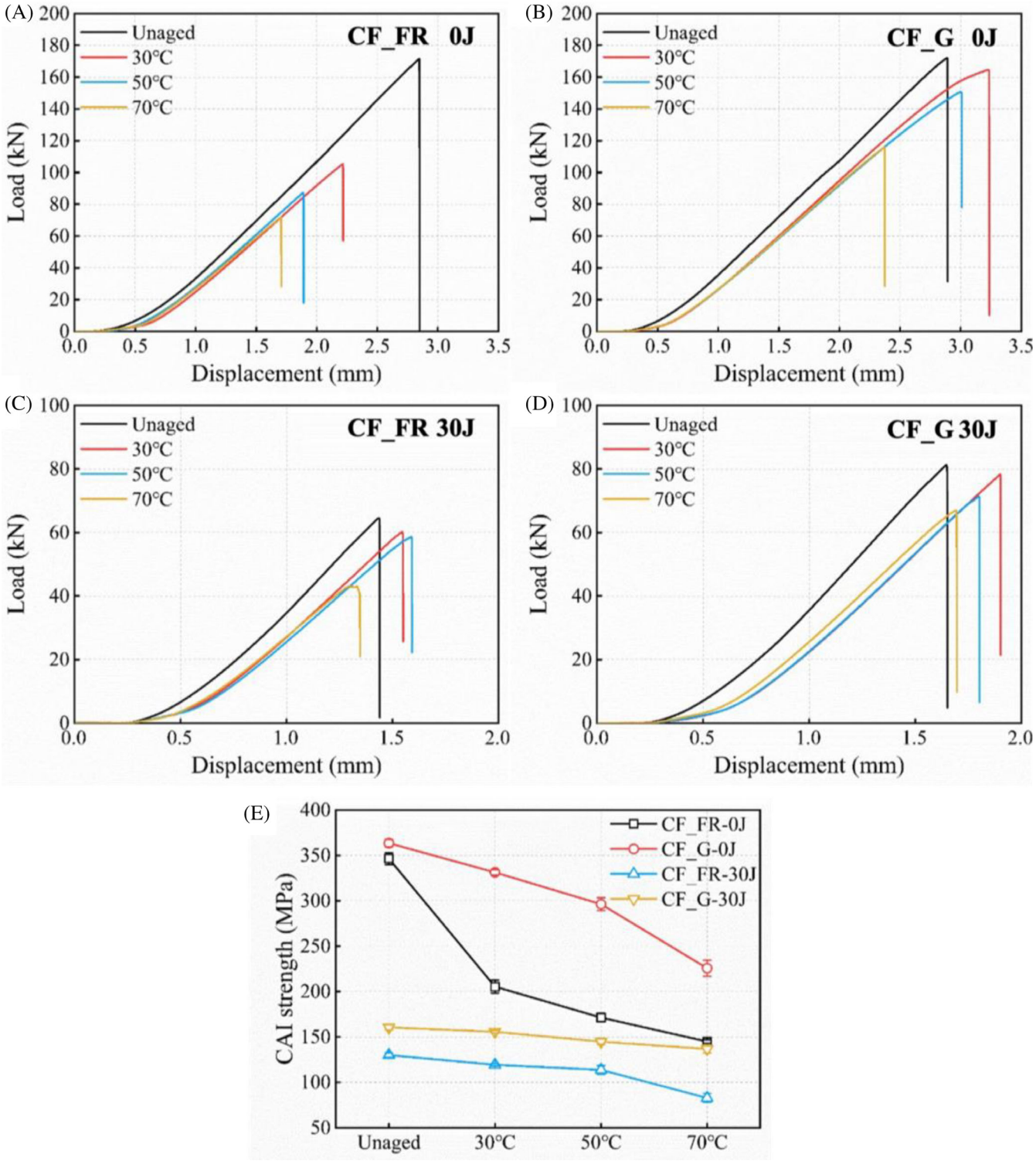

FIGURE 10 Load versus displacement curves under various hygrothermal conditions: (A) CF_FR for non-impact cases; (B) CF_G for non-impact cases; (C) CF_FR for 30 J; (D) CF_G for 30 J; and (E) CAI strength.

3.4 | CAI behavior

In order to assess the residual compression strength of the specimens, CAI tests were performed under both 30 J impact and non-impact conditions. It can be seen that all the curves show a similar trend in Figure 10A–D. Initially, the gap between the test fixture and the specimen was eliminated with a very small load, after which the compressive load increases linearly with the displacement. Upon reaching a certain load level, a sudden brittle failure of laminates is observed, accompanied by a significant drop in the load–displacement curve during the CAI tests. It is worth noting that the slopes of the load–displacement curves for the specimens conditioned in a hygrothermal aging environment exhibit a slight decrease, which suggests that matrix degradation due to moisture absorption during prolonged immersion in water reduces the CAI stiffness of the laminates.

Additionally, the compressive strengths of the two laminates were compared under non-impact conditions and 30 J of energy impact at different hygrothermal aging temperatures, as shown in Figure 10E. It is evident that the compressive strength of both laminates decreases as the hygrothermal aging temperature increases under all conditions, indicating a reduction in compressive damage resistance due to water absorption. Specifically, for non-impacted cases, the compressive strength of CF_FR under hygrothermal conditioning at 30–70°C is reduced by 40.7%–58.1% compared to unaged specimens. In contrast, the compressive strength of CF_G decreases by only 8.8%–37.9% under the same conditions. This observed difference in compressive strength can be attributed to the superior hygroscopicity of CF_FR, leading to more severe aging damage and noticeable degradation of laminate integrity, resulting in a more significant reduction in compressive strength. Under a 30 J impact, the CAI strength of CF_G and CF_FR immersed in a 70°C water bath shows a decrease of 36.3% and 14.8% respectively, compared to the unaged specimens. This difference may be due to the fact that delamination damage is more likely to occur in CF_FR at higher temperatures during hygrothermal aging, resulting in a more pronounced decrease in CAI strength. Therefore, it can be concluded that CF_FR are more susceptible to significant degradation in compressive strength and CAI strength after conditioning in a hygrothermal aging environment.

To analyze the failure mechanisms of CAI in both laminates under hygrothermal conditions, strain field distribution data was obtained from the surface during CAI tests using a VIC-2D system. Figure 11 shows the evolution of the longitudinal compressive strain for CF_FR and CF_G under compressive loading at three representative moments: A, B and C. Both types of laminates exhibit similar compressive failure mechanisms. During the CAI tests, the longitudinal compressive strain starts from the impact-damaged area and becomes noticeable when the load reaches point A. As the compressive load increases from A to B, the area with noticeable

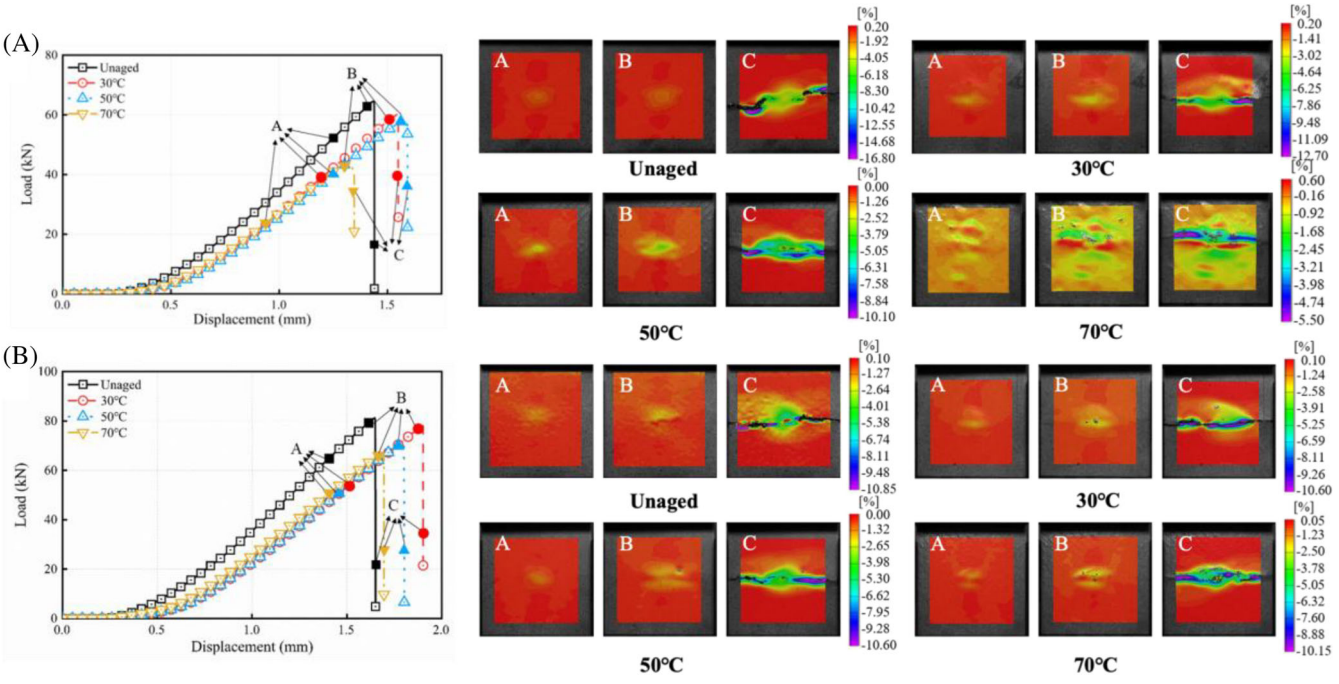

FIGURE 11 CAI behavior of (A) CF_FR at 30 J under different hygrothermal conditions and (B) CF_G at 30 J under different hygrothermal conditions.

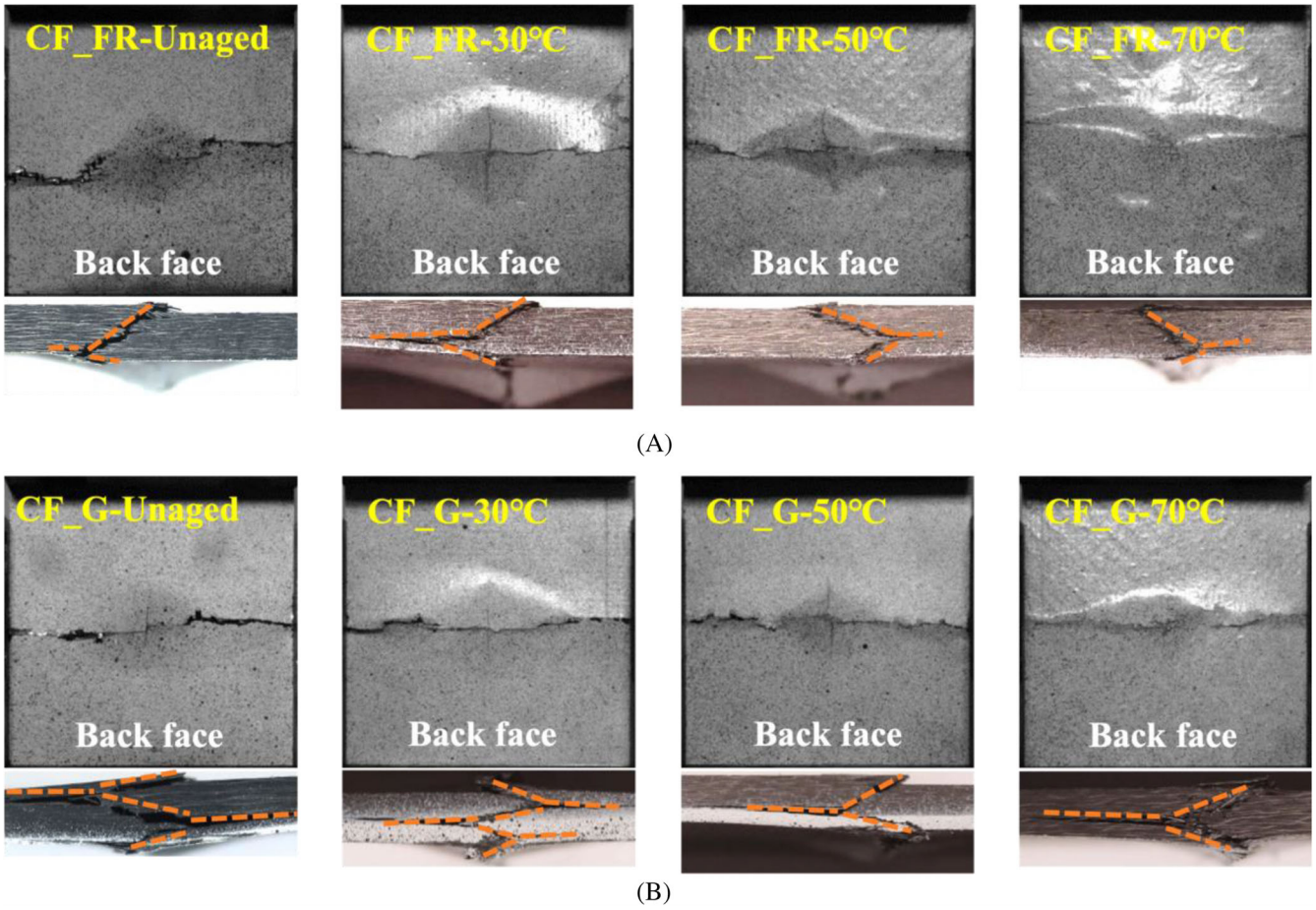

FIGURE 12 Compressive failure morphologies: (A) CF_FR under different hygrothermal conditions; (B) CF_G under different hygrothermal conditions.

longitudinal strain primarily propagates along the width direction due to the gradual expansion of impact-induced delamination. When the strains reach a critical level that causes compressive failure, the impact-damaged area suddenly becomes unstable, leading to a significant increase in compressive strain within a very short period, ultimately resulting in the overall compressive failure of the laminates. However, at a water bath temperature of 70°C, significant local deflection is observed on the surface of CF_FR under compressive loading, not only in the impact-damaged regions. This can be explained by the fact that CF_FR experiences substantial delamination damage and swelling when immersed in high-temperature water for prolonged periods, leading to a significant reduction in structural integrity. Consequently, pronounced local buckling occurs in the swollen regions under compressive loading, resulting in higher longitudinal compressive strains in the laminates.

Furthermore, the compressive failure morphologies of both laminates are presented in Figure 12. The temperature of the hygrothermal environment does not have a significant effect on the compressive damage morphology of the laminates after impact. The compressive failure in both laminates is characterized by transverse cracks propagating through the impact-damaged area, extrusion damage of the carbon fiber, and the formation of shear cracks through the thickness.

4 | CONCLUSIONS

In this paper, the effect of hygrothermal aging conditions on the mechanical behaviors of twill woven carbon fiber composite laminates with general (CF_G) and flame-retardant epoxy resin (CF_FR) thoroughly investigated. The findings revealed that CF_FR laminates experienced more significant aging damage due to their higher moisture absorption, leading to extensive swelling on the laminate surface and noticeable delamination within the internal microstructure compared to CF_G. Both types of laminates, when conditioned in various hygrothermal environments, exhibited a marked increase in peak force with rising aging temperatures, while the damaged area decreased, indicating a positive effect of hygrothermal

aging in reducing impact-induced damage. However, CF_FR was found to be more susceptible to impact-induced delamination, particularly at higher temperatures, as opposed to CF_G, which showed more concentrated fiber breakage due to lower moisture absorption. Additionally, CF_FR laminates suffered a more significant reduction in compressive strength and CAI strength after hygrothermal conditioning compared to CF_G, with a decrease of 36.3% for CF_FR and 14.8% for CF_G at 70°C, following an impact energy of 30 J. The study also highlighted the vulnerability of CF_FR to structural instability post-aging, as significant local buckling was observed in swollen regions under compressive loading, underscoring the severe impact of hygrothermal aging on the integrity and mechanical performance of these laminates.

ACKNOWLEDGMENTS

The authors gratefully acknowledge the support provided by the National Natural Science Foundation of China (Grant No. 12172130 and Grant No. 12302268), Primary Research & Development Plan of Jiangxi Province of China (Grant Nos. 20212BBE53016 and 20232ACB201007), and Guangdong Basic and Applied Basic Research Foundation (2022A1515110786).

DATA AVAILABILITY STATEMENT

Data sharing is not applicable to this article as no new data were created or analyzed in this study.

ORCID

Binbin Yin https://orcid.org/0000-0001-9660-8907

REFERENCES

1. Tuo H, Lu Z, Ma X, Xing J, Zhang C. Damage and failure mechanism of thin composite laminates under low-velocity impact and compression-after-impact loading conditions. *Compos B: Eng*. 2019;163:642-654.
2. Liu Y, Wang H, Ding H, Wang H, Bi Y. Effect of hygrothermal aging on compression behavior of CFRP material with different layups. *Compos B: Eng*. 2024;270:111134.
3. Imielińska K, Guillaumat L. The effect of water immersion ageing on low-velocity impact behaviour of woven aramid–glass fibre/epoxy composites. *Compos Sci Technol*. 2004;64:2271-2278.
4. Ghelli D, Minak G. Low velocity impact and compression after impact tests on thin carbon/epoxy laminates. *Compos B: Eng*. 2011;42:2067-2079.
5. Kostopoulos V, Baltopoulos A, Karapappas P, Vavouliotis A, Paipetis A. Impact and after-impact properties of carbon fibre reinforced composites enhanced with multi-wall carbon nanotubes. *Compos Sci Technol*. 2010;70:553-563.
6. Ge X, Zhang P, Zhao F, Liu M, Liu J, Cheng Y. Experimental and numerical investigations on the dynamic response of woven carbon fiber reinforced thick composite laminates under low-velocity impact. *Compos Struct*. 2022;279:114792.
7. Iqbal K, Khan S-U, Munir A, Kim J-K. Impact damage resistance of CFRP with nanoclay-filled epoxy matrix. *Compos Sci Technol*. 2009;69:1949-1957.
8. Zhou J, Lucas JP. Hygrothermal effects of epoxy resin. Part I: the nature of water in epoxy. *Polymer*. 1999;40:5505-5512.
9. Zhou J, Lucas JP. Hygrothermal effects of epoxy resin. Part II: variations of glass transition temperature. *Polymer*. 1999;40:5513-5522.
10. Aoki Y, Yamada K, Ishikawa T. Effect of hygrothermal condition on compression after impact strength of CFRP laminates. *Compos Sci Technol*. 2008;68:1376-1383.
11. Bao L-R, Yee AF. Moisture diffusion and hygrothermal aging in bismaleimide matrix carbon fiber composites—part I: uni-weave composites. *Compos Sci Technol*. 2002;62:2099-2110.
12. Berketis K, Tzetzis D, Hogg PJ. The influence of long term water immersion ageing on impact damage behaviour and residual compression strength of glass fibre reinforced polymer (GFRP). *Mater Des*. 2008;29:1300-1310.
13. Ray BC. Temperature effect during humid ageing on interfaces of glass and carbon fibers reinforced epoxy composites. *J Colloid Interface Sci*. 2006;298:111-117.
14. Lee MC, Peppas NA. Models of moisture transport and moisture-induced stresses in epoxy composites. *J Compos Mater*. 1993;27:1146-1171.
15. Vaddadi P, Nakamura T, Singh RP. Transient hygrothermal stresses in fiber reinforced composites: a heterogeneous characterization approach. *Compos Part A: Appl Sci Manuf*. 2003;34:719-730.
16. Ameer MH, Shaker K, Ashraf M, et al. Interdependence of moisture, mechanical properties, and hydrophobic treatment of jute fibre-reinforced composite materials. *J Text Inst*. 2017;108:1768-1776.
17. Schoeppner GA, Abrate S. Delamination threshold loads for low velocity impact on composite laminates. *Compos Part A: Appl Sci Manuf*. 2000;31:903-915.
18. Shyr T-W, Pan Y-H. Impact resistance and damage characteristics of composite laminates. *Compos Struct*. 2003;62:193-203.
19. Yang B, Chen Y, Lee J, Fu K, Li Y. In-plane compression response of woven CFRP composite after low-velocity impact: modelling and experiment. *Thin-Walled Struct*. 2021;158:107186.
20. Evci C, Gülgeç M. An experimental investigation on the impact response of composite materials. *Int J Impact Eng*. 2012;43:40-51.
21. Falcó O, Lopes CS, Sommer DE, Thomson D, Ávila RL, Tijs BHAH. Experimental analysis and simulation of low-velocity impact damage of composite laminates. *Compos Struct*. 2022;287:115278.
22. Fang L, Chu Y, Zhu X, et al. Low-velocity multiple impact damage characteristics and numerical simulation of carbon fiber/epoxy composite laminates. *Polym Compos*. 2024;45:2517-2531.
23. Yan H, Oskay C, Krishnan A, Xu LR. Compression-after-impact response of woven fiber-reinforced composites. *Compos Sci Technol*. 2010;70:2128-2136.
24. Rivallant S, Bouvet C, Abi Abdallah E, Broll B, Barrau J-J. Experimental analysis of CFRP laminates subjected to compression after impact: the role of impact-induced cracks in failure. *Compos Struct*. 2014;111:147-157.

25. Sun XC, Hallett SR. Failure mechanisms and damage evolution of laminated composites under compression after impact (CAI): experimental and numerical study. *Compos Part A: Appl Sci Manuf*. 2018;104:41-59.
26. Tuo H, Lu Z, Ma X, Zhang C, Chen S. An experimental and numerical investigation on low-velocity impact damage and compression-after-impact behavior of composite laminates. *Compos B: Eng*. 2019;167:329-341.
27. Li H, Yu Z, Tao Z, Liu K. Experimental investigations on the repeated low velocity impact and compression-after-impact behaviors of woven glass fiber reinforced composite laminates. *Polym Compos*. 2024;45:1884-1897.
28. Khashaba UA, Othman R. Low-velocity impact of woven CFRE composites under different temperature levels. *Int J Impact Eng*. 2017;108:191-204.
29. Raponi E, Sergi C, Boria S, Tirillò J, Sarasini F, Calzolari A. Temperature effect on impact response of flax/epoxy laminates: analytical, numerical and experimental results. *Compos Struct*. 2021;274:114316.
30. Karahan M, Gül H, Ivens J, Karahan N. Low velocity impact characteristics of 3D integrated core sandwich composites. *Text Res J*. 2012;82:945-962.
31. Karahan M, Karahan N. Effect of weaving structure and hybridization on the low-velocity impact behavior of woven carbon-epoxy composites. *Fibres Text East Eur*. 2014;33:212-222.
32. Othman R, Khashaba UA, Almitani KH. Compression after impact of CFRE composites immersed in distilled water. *Int J Crashworth*. 2020;26:490-500.
33. Zhong Y, Joshi SC. Impact behavior and damage characteristics of hygrothermally conditioned carbon epoxy composite laminates. *Mater Des 1980–2015*. 2015;65:254-264.
34. Dogan A, Arman Y. The effect of hygrothermal aging and UV radiation on the low-velocity impact behavior of the glass fiber-reinforced epoxy composites. *Iran Polym J*. 2019;28:193-201.
35. Karahan M, Karahan N. Influence of weaving structure and hybridization on the tensile properties of woven carbon-epoxy composites. *J Reinf Plast Compos*. 2013;33:212-222.

How to cite this article: Zhong J, Ma J, Sun W, Lei Z, Yin B. Hygrothermal aging effects on the mechanical behaviors of twill-woven carbon fiber composite laminates with flame-retardant epoxy resin. *Polym Compos*. 2025;46(2):1737-1752. doi:10.1002/pc.29070